ISH Journal of Hydraulic Engineering
Publication details, including instructions for authors and subscription information:
http://www.tandfonline.com/loi/tish20

Multi-variable regression models for prediction of discharge and approach velocity coefficients in flow measurement flumes with compound cross-section

Issam A. Al-Khatib[a] & Khaled A. Abaza[b]

[a] Institute of Environmental and Water Studies, Birzeit University, West Bank, Palestine

[b] Department of Civil Engineering, Birzeit University, West Bank, Palestine

Published online: 29 Sep 2014.

To cite this article: Issam A. Al-Khatib & Khaled A. Abaza (2015) Multi-variable regression models for prediction of discharge and approach velocity coefficients in flow measurement flumes with compound cross-section, ISH Journal of Hydraulic Engineering, 21:1, 65-84, DOI: 10.1080/09715010.2014.963175

To link to this article: http://dx.doi.org/10.1080/09715010.2014.963175

ISH Journal of Hydraulic Engineering, 2015
Vol. 21, No. 1, 65–84, http://dx.doi.org/10.1080/09715010.2014.963175

Multi-variable regression models for prediction of discharge and approach velocity coefficients in flow measurement flumes with compound cross-section

Issam A. Al-Khatib[a]* and Khaled A. Abaza[b]

[a]*Institute of Environmental and Water Studies, Birzeit University, West Bank, Palestine;* [b]*Department of Civil Engineering, Birzeit University, West Bank, Palestine*

(*Received 4 March 2014; accepted 19 August 2014*)

In this paper, two multi-variable regression models have been developed to predict the discharge and approach velocity coefficients from relevant independent variables. The regression models are developed based on relevant experimental data obtained from testing nine different flow measurement long-throated flumes with symmetrical rectangular compound cross-sections. The long-throated flume was used in the compound cross-section to experimentally estimate the discharge and approach velocity coefficients using mainly head measurements and cross-section dimensions as required by the stage-discharge equations. The independent variables used in predicting the two coefficients represent dimensionless parameters defined using the gauged head at the head measurement section, floodplain depth, length of throat in the direction of flow, and cross-section geometry at the control section. Several statistically-based analyses were performed to verify the reliability of the developed multi-variable regression models. All deployed analyses have indicated that the two regression models are associated with high predictive strength. Therefore, the main contribution of this paper is the development of regression-based models to predict the discharge and approach velocity coefficients that can be used in conjunction with stage-discharge equations to estimate the flow in a symmetric rectangular channel with compound cross-section.

Keywords: flow measurement; flumes; discharge coefficient; approach velocity coefficient; discharge rating

1. Introduction

Generally, natural rivers and streams are comprised of two-stage channels defined as flood plains and main channel. The ability to predict discharge in compound open channels is highly important from hydraulic and irrigation engineering viewpoint considering various hydrological applications. It can help engineers and practitioners to provide essential information regarding the construction of hydraulic structures, water resources planning, water and sediment budget analysis, hydrologic modeling, reservoir operation, flood mitigation, and as far as planning for effective control and preventive measures (Al-Khatib et al. 2012, 2013; Ghimire and Reddy 2010; Sahu et al. 2011; Unal et al. 2010; Van Prooijen et al. 2005).

Several types of structures have been used for a long time in performing discharge measurement in open channels such as flumes, gates, and weirs (Boiten 2002; Vatankhah and Mahdavi 2012). Examples of such structures used in the past two decades are the Parshall flumes developed as simple devices for flow measurements in open channels (Heiner and Barfuss 2011), the broad crested weir considered as a flat-crested structure with a crest length large compared to the flow thickness (Gonzalez and Chanson 2007), and the broad-crested weirs and long-throated flumes are also used for open channel flow measurements (Clemmens et al. 1984). The long-throated flumes and weirs provide cost-effective, practical and flexible capabilities for measuring discharge in open channel systems as used in irrigation. The main advantages associated with using these structures are the low construction cost, adaptability to a variety of channel types, minimal head loss, and ability to measure wide ranges of flows with custom-designed structures (Sahu et al. 2011; Wahl et al. 2005). In addition, special computer programs can be used to design and calibrate flumes such as the WinFlume (Wahl et al. 2000). The design procedure and hydraulic theory for these flow measurement structures have been considerably presented in the research titled “water measurement with flumes and weirs” (Clemmens et al. 2001).

The discharge coefficient (C_d) and approach velocity coefficient (C_v) of long-throated flumes depend on several parameters including main channel width, step height and throat length. In this research paper, the effects of these geometric dimensions on the values of discharge coefficient and approach velocity coefficient will be investigated using a series of laboratory experiments carried out in a flow measurement flume of a symmetrical rectangular compound cross-section. In addition, multiple-variable regression techniques will be used to develop models that can predict the discharge and approach velocity coefficients (C_d and C_v) from relevant geometric parameters. The predicted coefficients can then be used to estimate the corresponding channel discharges.

*Corresponding author. Email: ikhatib@birzeit.edu

1.1. *Stage-discharge equation*

The long throated flumes have almost parallel flow in the approach channel where the flow depth is measured. Therefore, the pressure distribution is assumed to be hydrostatic, and existing theory based on critical flow can be used to measure open channel discharges. The critical flow condition can be generated through a control section with known dimensions using an appropriate critical flow device such as the long throated flume. The discharge through the critical section is only a function of the section shape, and the upstream potential energy as indicated by the water level upstream from the critical flow structure. The presence of critical flow in the control section will essentially prevent the downstream flow conditions from affecting the flow through the critical section, therefore, the discharge can be computed as a function of the measured upstream head. The critical flow devices include, for example, the sharp-crested weirs, broad-crested weirs, and a wide variety of flumes. The specific relationship between the discharge and upstream head must be defined when using a critical flow device for flow measurement. Also, the range over which this relationship is applicable must be defined (Clemmens et al. 2001; Emamgholizadeh and Assare 2008).

The plan view, longitudinal profile, head measurement and control sections for the developed flow measurement structure are shown in Figure 1. The head-discharge equations can be derived for long throated flumes based on the energy equation between the head measurement section and the control section while assuming the energy losses are neglected, velocity distributions are kept uniform, and streamlines are all straight and parallel to each other. Then, the procedure outlined by many authors can be used to derive the head-discharge equations (Al-Khatib 1989, 1993, 1999; Bos and Reinink 1981; Bos et al. 1984; Clemmens et al. 1987 Göğüş and Al-Khatib 1995; Göğüş et al. 2006). In this paper, only the final results of the head-discharge equations of flumes with symmetrical rectangular compound cross section will be presented for two cases as follows:

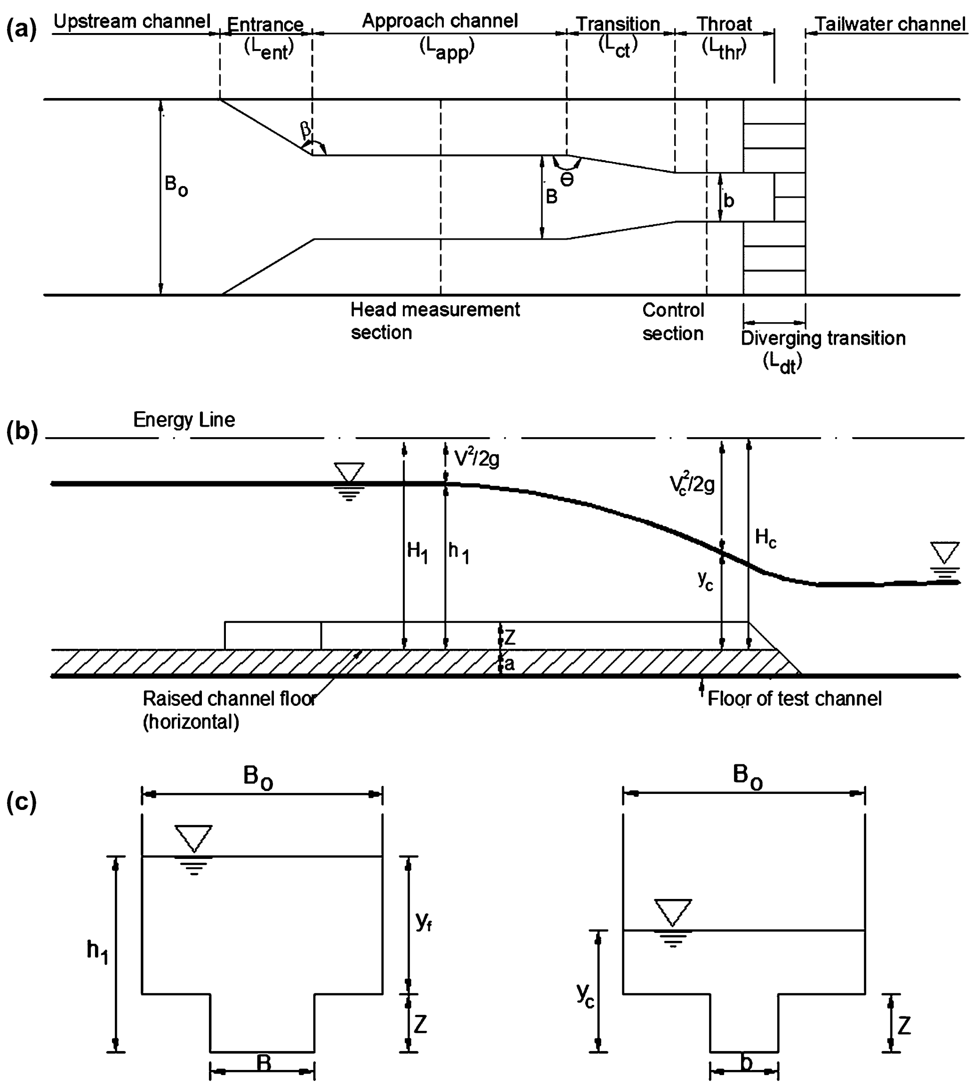

Figure 1. Definition sketch of models used in theoretical analysis: (a) plan view; (b) longitudinal profile; (c) head measurement and control sections.

Case 1 ($h_1 \leq Z$, $y_c < Z$)

This is the case where flow occurs only through the lower part of the compound cross section ($h_1 \leq Z$, $y_c < Z$), where h_1 = gauged head at the head measurement section; Z = step height; y_c = critical water depth at control section. For this case, the equations of stage-discharge, discharge coefficient, and approach velocity coefficient can be obtained as indicated by Equations (1)–(3), respectively.

$$Q = \frac{2}{3} C_d C_v b \left(\frac{2}{3} g\right)^{\frac{1}{2}} h_1^{\frac{3}{2}} \tag{1}$$

$$C_d = \frac{3}{2} \frac{Q}{b(\frac{2}{3}g)^{\frac{1}{2}} H_1^{\frac{3}{2}}} \tag{2}$$

$$C_v = \left(\frac{H_1}{h_1}\right)^{\frac{3}{2}} \tag{3}$$

where Q = flow rate ($Q = A_c V_c$); and $A_c = by_c$ = flow area at the control section; b = bottom width of the control section; V_c = average critical velocity; h_1 = gauged head at the head measurement section; H_1 = the total energy head of the flow at the head measurement section; and g = acceleration due to gravity. The discharge coefficient (C_d) accounts for idealized assumptions at the head measurement and control sections in the stage-discharge equation such as for energy losses, velocity distributions, and streamline curvature. However, the approach velocity coefficient (C_v) corrects for the neglect of the velocity head at the head measurement section as it is not possible to measure the energy head (H_1) directly in an open channel. Therefore, the common practice is to relate the flow rate to the upstream still-referenced water level (h_1) using the approach velocity coefficient (C_v) as defined in Equation (3).

Case 2 ($h_1 > Z$, $y_c > Z$)

In this case, flow occurs through the compound cross-section, so that the water depth at the control section (i.e. the critical depth) is greater than the set height (Z). The area of the flow at the control section is obtained using Equation (4).

$$A_c = bZ + (y_c - Z)B_o \tag{4}$$

where B_o = top width of the head measurement section. The equations of stage-discharge, discharge coefficient, and approach velocity coefficient are presented in Equations (5)–(7), respectively.

$$Q = C_d C_v \left(\frac{g}{B_o}\right)^{\frac{1}{2}} \left[bZ + B_o\left(\frac{2}{3}h_1 - \frac{bZ}{3B_o} - \frac{2Z}{3}\right)\right]^{\frac{3}{2}} \tag{5}$$

$$C_d = \frac{Q\left(\frac{B_o}{g}\right)^{\frac{1}{2}}}{\left[bz + B_o(\frac{2}{3}H_1 - \frac{bZ}{3B_o} - \frac{2Z}{3})\right]^{\frac{3}{2}}} \tag{6}$$

$$C_v = \left[\frac{bz + B_o(\frac{2}{3}H_1 - \frac{bZ}{3B_o} - \frac{2Z}{3})}{bz + B_o(\frac{2}{3}h_1 - \frac{bZ}{3B_o} - \frac{2Z}{3})}\right]^{\frac{3}{2}} \tag{7}$$

The general idea of the proposed approach is to measure the upstream water level (h_1), estimate the values of C_d and C_v using empirical models developed from regression techniques**,** and then compute the discharge using either Equations (1) or (5). Consequently, a major contribution of the proposed approach is the generation of predictive empirical models for estimating the discharge and approach velocity coefficients which can be used in conjunction with stage-discharge equations to estimate the discharge in a symmetric rectangular channel with compound cross-section.

2. Experimental setup and experiments

The experiments were conducted in the Hydromechanics Laboratory of the Civil Engineering Department, Middle East Technical University, Ankara-Turkey, using a glass walled laboratory flume with 0.70 m deep, 0.287 m wide and 11.0 m long. The compound rectangular open channel was constructed from plexiglass with two flood plains added in the manner shown in Figure 1. A symmetrical cross-section was thus created with a center channel placed almost to the mid-length of the main channel system. Figure 2 shows two actual photos of the overall experimental setup.

The original floor level was raised by a = 4 cm and kept horizontal up to the end of the throat length. Then, the diverging transition was formed towards the tailwater channel. By doing this, an elevation difference of a = 4 cm was created between the floor of test channel and the invert of flume to avoid submerged flow downstream of the throat. The constant diverging transition slope (1 vertical: 3 horizontal) is attained over the total width of the tailwater channel by keeping the length of the sidewalls of the throat at specified values.

The dimensions of the various models used in the experiments are given in Table 1. The symbols used in the description of model types, BiZi (i = 1, 2, 3), correspond to the width and height of the main channel at the head measurement section, respectively. The volumetric flow rate was measured with a rectangular sharp crested weir. The point gauge was used along the centerline of the model for head measurement at the head measurement section. The bottom elevation of the flume was used as reference.

(a)

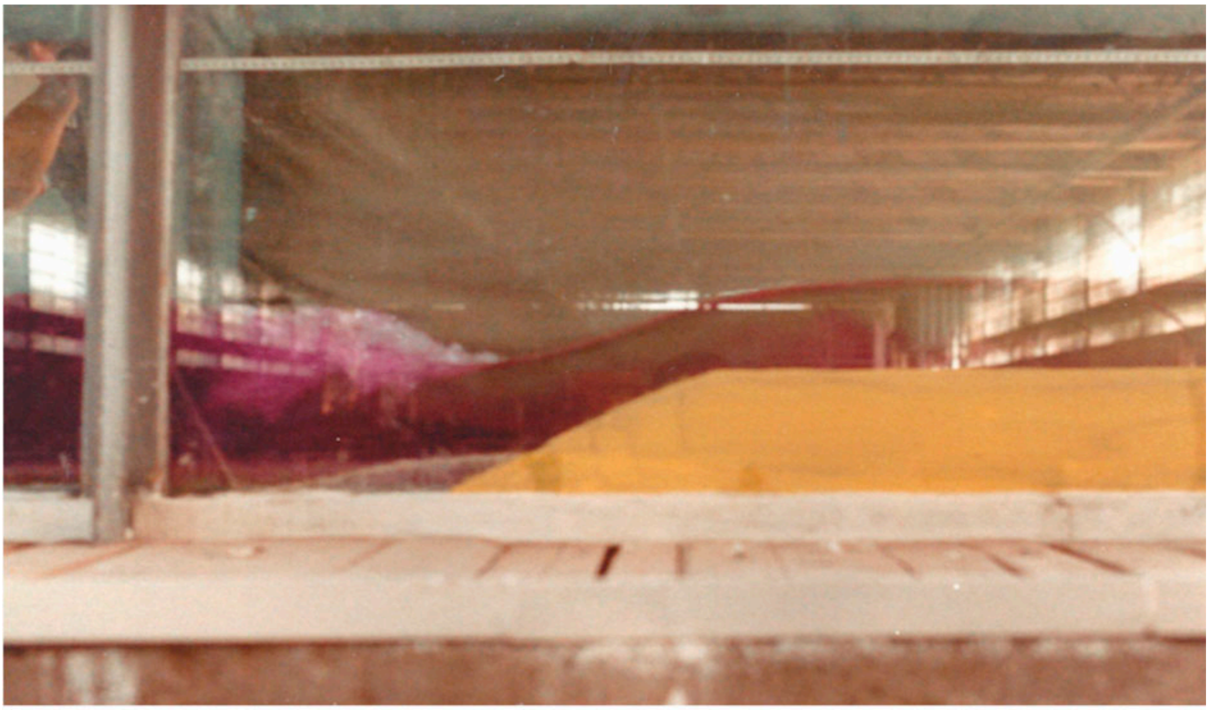

(b)

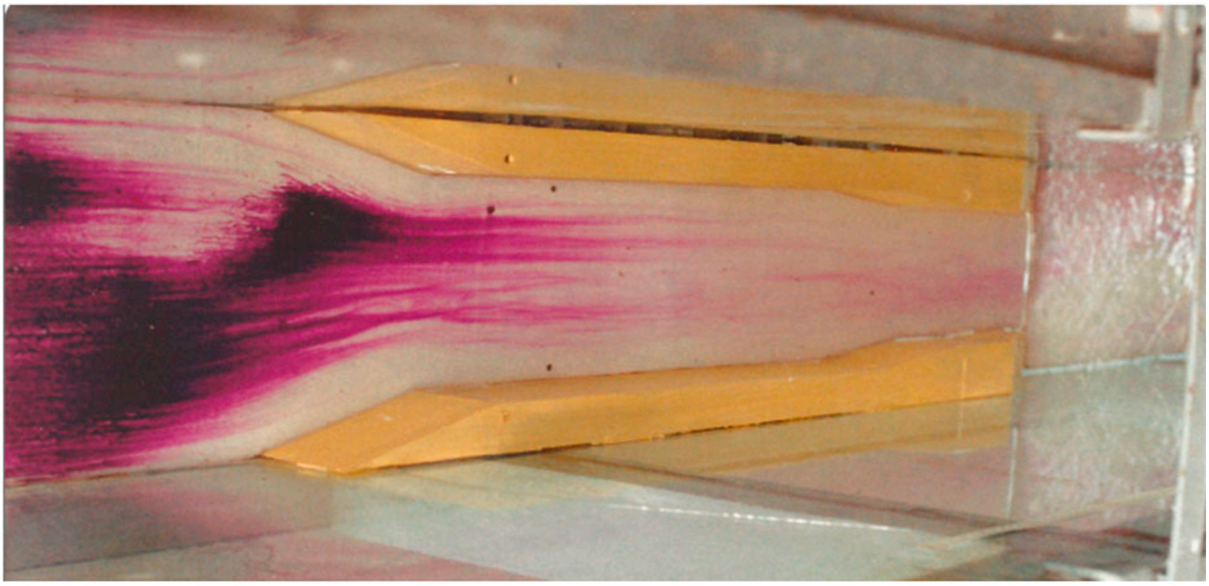

Figure 2. Photographs of model type B3Z3. (a) model side view, (b) model top view. [To view a colour version of this figure, see the online version of this Journal.]

Table 1. Models used in experiments.

Types of models	b (cm)	B (cm)	Z (cm)	L_{ent} (cm)	L_{thr} (cm)	L_{dt} (cm)	b/B	b/B_o
B1Z1	6	10	2	37.4	18	16.5	0.600	0.209
B1Z2	6	10	6	37.4	30	28.5	0.600	0.209
B1Z3	6	10	10	37.4	42	40.5	0.600	0.209
B2Z1	11	15	2	27.4	18	16.5	0.733	0.383
B2Z2	11	15	6	27.4	30	28.5	0.733	0.383
B2Z3	11	15	10	27.4	42	40.5	0.733	0.383
B3Z1	16	20	2	17.4	18	16.5	0.800	0.557
B3Z2	16	20	6	17.4	30	28.5	0.800	0.557
B3Z3	16	20	10	17.4	42	40.5	0.800	0.557

Note: B_{o} = 28.7 cm; L_{app} = 60 cm; L_{ct} = 16 cm; β = 166 degrees; and θ = 173 degrees.

For a selected model type BiZi, a wide range of discharges obtained from the constant head storage tank of the laboratory was examined. At the flow depth measurement section of the model, which was located at the midsection of the approach channel for all tested models, the depth of the flow above the crest level was measured when the tailwater gate of the flume was fully open (free flow measurements).

3. Presentation and discussion of results

In this section, the experimentally estimated discharge and velocity coefficients will be graphically presented and investigated in relation to relevant geometric parameters.

3.1. *Discharge coefficient (C_d)*

The impact of two dimensionless parameters on the discharge coefficient (C_d) will be investigated in relation to the control cross-section geometry, namely, bottom width (b) and step height (Z). The two parameters are the ratio h_1/L_{thr}, and depth ratio of y_f/h_1.

3.1.1. *Variation of discharge coefficient with h_1/L_{thr}*

In the literature, the discharge coefficient (C_d) is normally related to the dimensionless ratio H_1/L_{thr} (Bos 1977, 1989; Bos and Reinink 1981; Emamgholizadeh and Assare 2008). But for practical purposes, it is preferred to relate it to the dimensionless ratio h_1/L_{thr} as it is difficult to compute H_1 directly at the head measurement section, while h_1 can be directly measured. The experimentally estimated C_d values are determined using Equations (2) and (6) based on the measured discharge and cross-section geometric dimensions and are presented in Figures 3–9 as a function of h_1/L_{thr}.

3.1.1.1. The effect of variable bottom width (b). The main observation obtained from Figures 3–9 is that the value of discharge coefficient (C_d) increases with the increase in the value of h_1/L_{thr}. The effect of the bottom width of the control section (b) on the discharge coefficient is investigated by comparing the C_d values obtained from the experiments carried out on the nine tested models with varying control section bottom width (b) and constant step height (Z). The values of C_d for three different b values are plotted as a function of h_1/L_{thr} while keeping the step height constant as shown in Figures 3–5. Figure 4 depicts the C_d values for a 6 cm constant step height (Z) while using three different values for the bottom width (b = 6, 11, 16 cm). It can be noticed from Figure 4 that below a 0.5 critical h_1/L_{thr} value, the C_d values show unclear trend for the 3 tested models (B1Z2, B2Z2, B3Z3). However, the C_d values associated with a critical h_1/L_{thr} value greater than 0.5, it is clear that the C_d values associated with B1Z2 model are smaller than the values associated with B2Z2 model, which are in turn smaller than the values for B3Z2 model. This trend is also true for the models presented in Figure 5 with a 0.45 critical (h_1/L_{thr}) value. The models presented in Figure 3 show a trend wherein B3Z1 model is falling between the other two models. Therefore, it can generally be concluded that as the control section bottom width (b) is increased, it will result in an increase in the value of discharge coefficient (C_d) considering a constant step height (Z).

From these figures, it can clearly be seen that the data points of model types B1Z1, B1Z2 and B1Z3 fall far below those of other model types. On the other hand, the (C_d) values shown in Figures 3–5 for model types B2Zi and B3Zi (i = 1, 2, 3) fall very close to each other for the same h_1/L_{thr} values.

3.1.1.2. The effect of variable step height (Z). Figures 6–8 are developed to investigate the effect of step height (Z) on C_d values as a function of h_1/L_{thr} for models with constant throat width (b). The general trend that can be noted from Figure 6 is that the C_d values associated with B1Z1 model are smaller than the corresponding values associated with B1Z2 model,

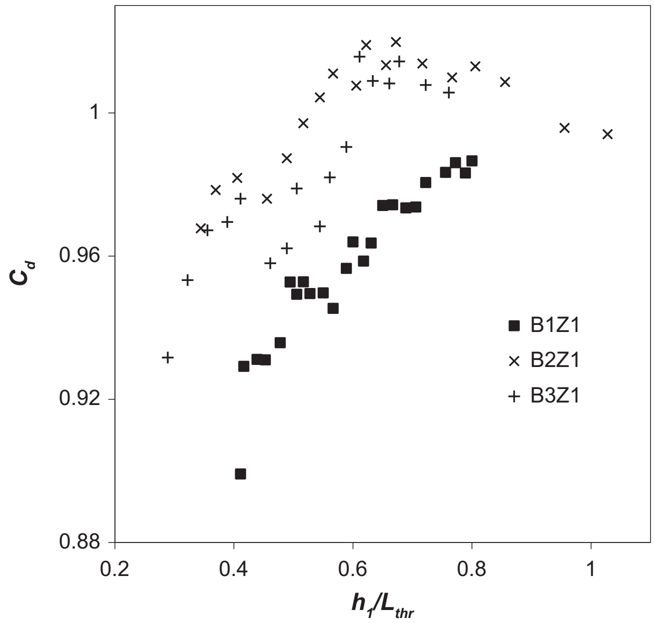

Figure 3. C_d vs. h_1/L_{thr} for varying bottom width of the control section and constant step height (Z = 2 cm).

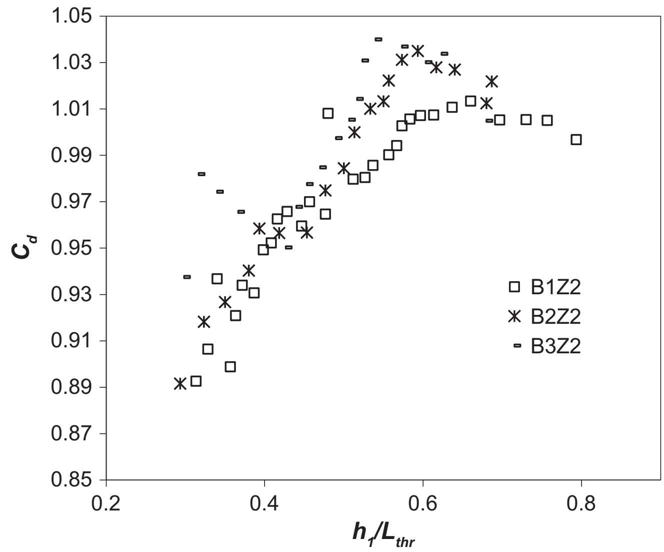

Figure 4. C_d vs. h_1/L_{thr} for varying bottom width of the control section and constant step height (Z = 6 cm).

which are in turn smaller than the values for B1Z3 model provided the h_1/L_{thr} ratio is larger than about 0.5. The trend becomes unclear for (h_1/L_{thr}) values below 0.5. Figures 7 and 8 show a trend similar to the one indicated by Figure 6 with corresponding critical h_1/L_{thr} values of 0.55 and 0.45, respectively. Therefore, it can be concluded that the C_d value increases as the step height (Z) increases considering constant control section width (b) and about 0.5 critical h_1/L_{thr} value. Figure 9 presents the C_d values vs. h_1/L_{thr} for all 9 tested models. As a general trend, the C_d value increases as the h_1/L_{thr} ratio increases up to a certain point, then it becomes almost independent of h_1/L_{thr}.

3.1.2. *Variation of discharge coefficient with y_f/h_1*

The effect of the y_f/h_1 ratio on the discharge coefficient (C_d) will be investigated in this section. In order to have a floodplain discharge, the flow should occur through the entire compound cross-section with the flow critical depth being greater than the step height of the rectangular compound cross-section ($y_c > Z$). The floodplain depth (y_f) equals to the difference between the head at upstream head measurement section (h_1) and step height of model cross-section (Z) (i.e. $y_f = h_1 - Z$).

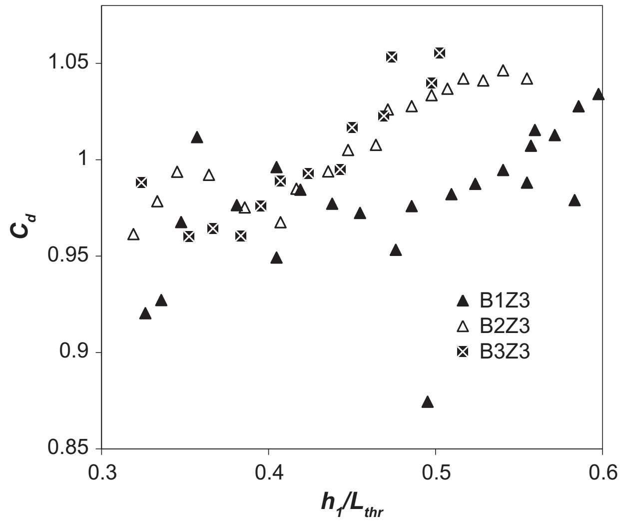

Figure 5. C_d vs. h_1/L_{thr} for varying bottom width of the control section and constant step height (Z = 10 cm).

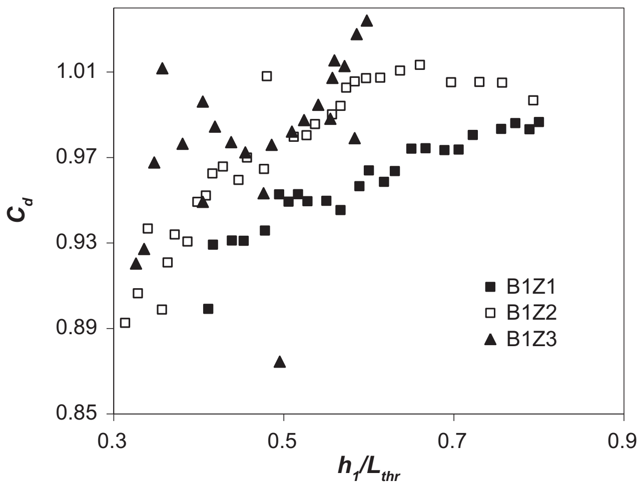

Figure 6. C_d vs. h_1/L_{thr} for varying step height and constant bottom width of the control section (b = 6 cm).

3.1.2.1. The effect of variable bottom width (b). The effect of the bottom width (b) on the discharge coefficient is investigated by comparing the C_d values obtained from the experiments carried out on the tested models with varying b and constant Z. The C_d values for the three different b values are plotted as a function of y_f/h_1 while keeping Z constant in Figures 10–12. For a step height of Z = 2 cm, there is no clear trend of the C_d versus y_f/h_1 as indicated by Figure 10. However, for a step height of Z = 6 (Figure 11) and Z = 10 cm (Figure 12), the C_d value increases as b value increases after exceeding the critical y_f/h_1 value of 0.58 for models BiZ2 and 0.47 for models BiZ3 (i = 1, 2, 3), respectively.

3.1.2.2. *The effect of variable step height (Z)*

The effect of the step height on the discharge coefficient will be examined by plotting C_d values as a function of y_f/h_1 for different step heights (Z) while keeping the width of the control section (b) constant (Figures 13–15). It can be noted from Figures 13–15 that the same C_d value can be obtained for the three models provided in each figure but using different y_f/h_1 values. This means the variation in the step height has minor effect on the discharge coefficient. It can be noticed that the same C_d value corresponds to the highest y_f/h_1 value for models with smallest step height (i.e. BiZ1, i = 1, 2, 3) and to the lowest y_f/h_1 value for models with the highest step height (i.e. BiZ3, i = 1, 2, 3). However, for the 3 models with medium step height (i.e. BiZ2, i = 1, 2, 3), the y_f/h_1 value falls between the lowest and highest y_f/h_1 value considering the same C_d value. This trend can be generalized for all nine tested models as shown in Figure 16. Also, it can to some extent be concluded from Figure 16 that the C_d value increases as the y_f/h_1 value increases.

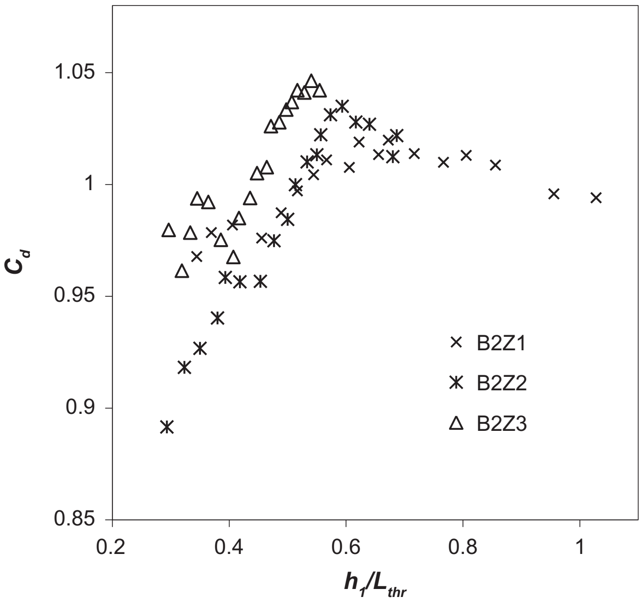

Figure 7. C_d versus $h_1/L_{\rm thr}$ for varying step height and constant bottom width of the control section (b = 11 cm).

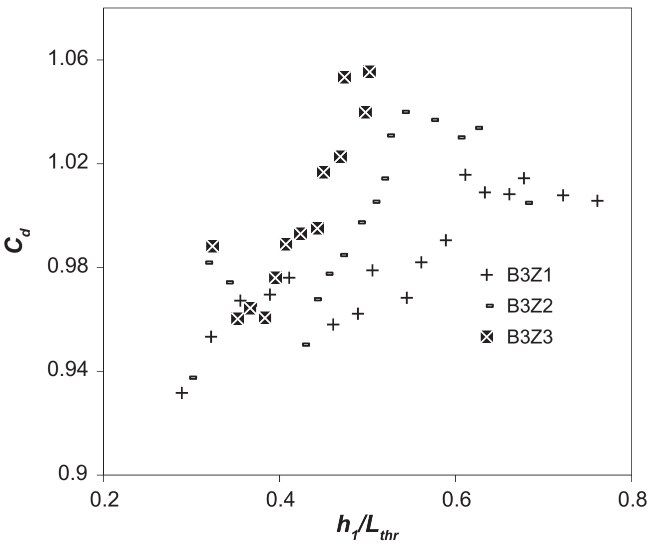

Figure 8. C_d vs. $h_1/L_{\rm thr}$ for varying step height and constant bottom width of the control section (b = 16 cm).

For the data of the models having b = 2 cm, model B1Z3 has larger C_d values compared to those associated with B1Z1 and B1Z2 models. The same trend can be noticed for B2Zi and B3Zi models (i = 1, 2, 3) meaning the C_d values increase as the step height increases for a fixed y_f/h_1 value.

3.2. *Approach velocity coefficient (C_v)*

The impact of two dimensionless parameters on the approach velocity coefficient (C_v) will be investigated in relation to the control cross-section geometry, namely, bottom width (b) and step height (Z). The two parameters are the area ratio (R_1) and depth ratio (y_f/h_1).

3.2.1. *Variation of approach velocity coefficient with R_1*

Because the discharge is mainly determined by the area of flow at the control section as defined in Equations (1) and (5) and the related approach velocity is also determined by the area of flow at the gauging station, it was found to be

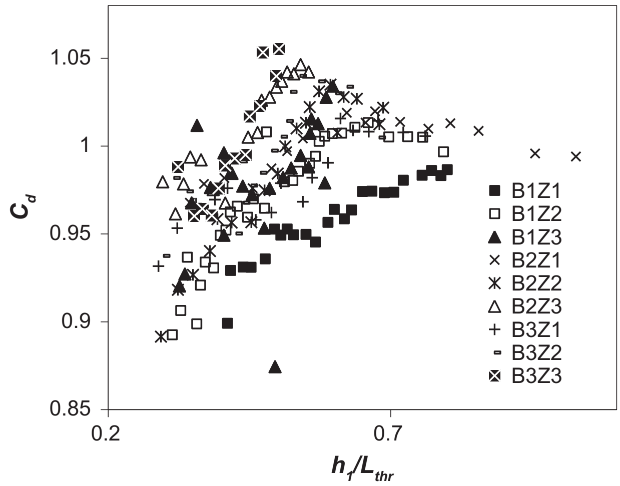

Figure 9. C_d vs h_1/L_{thr} for all tested models.

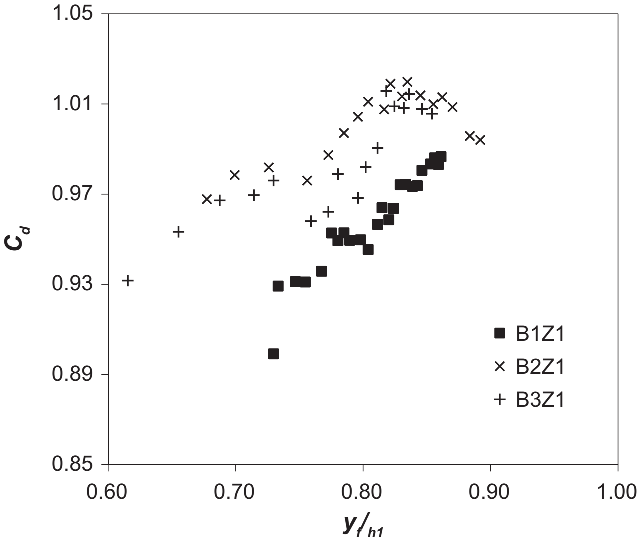

Figure 10. C_d vs. y_f/h_1 for varying bottom width of the control section and constant step height (Z = 2 cm).

convenient to correlate C_v to the area ratio (R_1) as defined in Equation (8) (Bos 1989). In this ratio, A^* is the imaginary projected area of flow at the control section and it depends on the relationship among the control depth (h_1), critical depth (y_c), and step height (Z) as indicated by Equations (9) and (10).

$$R_1 = \sqrt{\propto} C_d A^* / A_1 \tag{8}$$

where α = energy correction coefficient taken to be 1.04 in this study (Al-Khatib 1989; Bos 1989).

For $h_1 \leq Z$, $y_c < Z$,

$$A^* = bh_1 \quad \text{and} \quad A_1 = Bh_1 \tag{9}$$

For $h_1 > Z$, $y_c > Z$,

$$A^* = bZ + B_o(h_1 - Z) \quad \text{and} \quad A_1 = BZ + B_o(h_1 - Z) \tag{10}$$

The experimental results of all tested models related to C_v were presented as a function of R_1 and plotted in Figure 17. It can be noted that the variations in the step height (Z) and bottom width of the control section (b) do not have any significant impact on the coefficient of approach velocity (C_v).

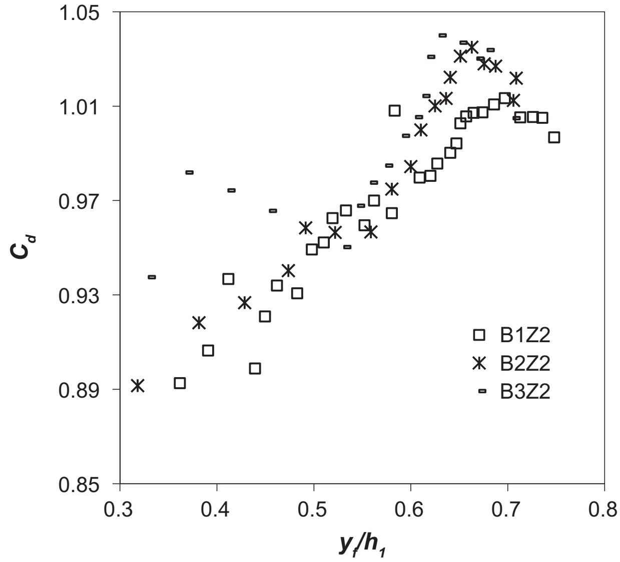

Figure 11. C_d vs. y_f/h_1 for varying bottom width of the control section and constant step height (Z = 6 cm).

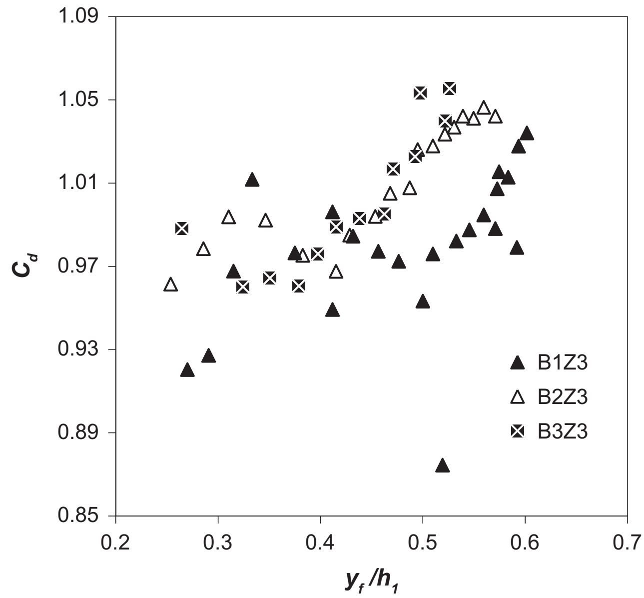

Figure 12. C_d vs. y_f/h_1 for varying bottom width of the control section and constant step height (Z = 10 cm).

3.2.2. *Variation of approach velocity coefficient with y_f/h_1*

In this section, the impact of the y_f/h_1 ratio on the approach velocity coefficient (C_v) will be examined. In this regard, both the control section bottom width (b) and step height (Z) will be considered.

3.2.2.1. The effect of variable bottom width (b). Figures 18–20 show the variation of (C_v) for models having constant step heights (Z) but variable control section bottom width (b). Figure 18 shows unclear trend for the variation of the velocity coefficient (C_v) with increasing control section bottom width considering a constant step height of 2 cm. However, Figures 19 and 20 show that as the bottom width increases, the C_v value also increases past a critical y_f/h_1 value of 0.6 for BiZ2 models and 0.43 for BiZ3 models (i = 1, 2, 3), respectively. This means that the effect of the lower weir crest width on C_v becomes more significant with the increase in step height.

3.2.2.2. The effect of variable step height (Z). Figures 21–23 show the variation of C_v with y_f/h_1 for models having constant bottom width of the control section but varying step height. From Figure 21, it can be noted that the same C_v value can be obtained using a constant bottom width (b) but with 3 different step heights (Z). This means the variation in the

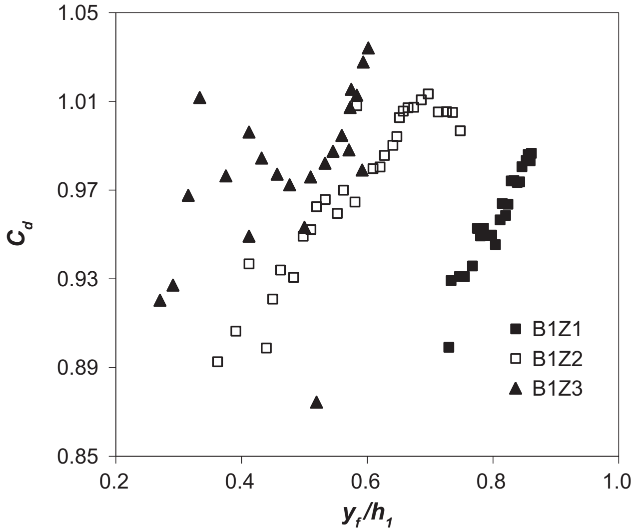

Figure 13. C_d vs. y_f/h_1 for varying step height and constant bottom width of the control section (b = 6 cm).

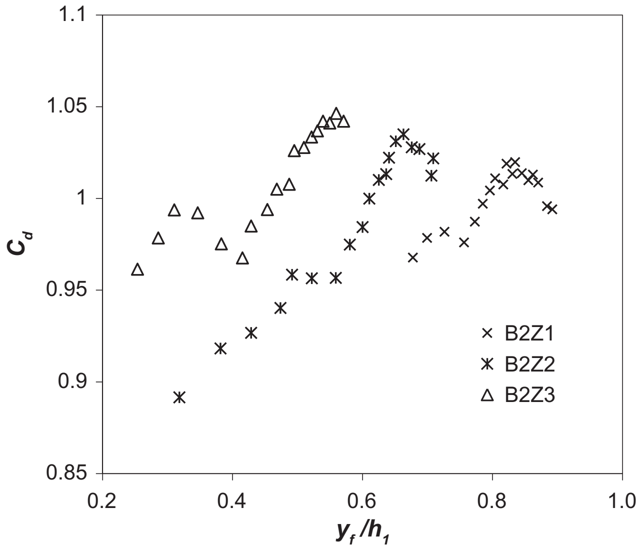

Figure 14. C_d vs. y_f/h_1 for varying step height and constant bottom width of the control section (b = 11 cm).

step height has minor effect on the approach velocity coefficient. It can be noticed that the same C_v value is associated with a higher y_f/h_1 ratio and a lower step height (Z) such as in the case of B1Z1 model or it is associated with a lower y_f/h_1 ratio and a higher step height (Z) such as in the case of B1Z3 model. It can also be noted from Figure 21 that the smallest variation in the C_v values take place between models B1Z2 and B1Z3. Similar observations can be made from Figures 22 and 23. Figure 24 depicts the C_v values obtained from all 9 tested models. It can be noted from Figure 24 that the highest y_f/h_1 ratio is associated with B1Z1 model (i.e. lowest bottom width and lowest step height) while the lowest y_f/h_1 ratio is associated with model B3Z3 (i.e. highest bottom width and highest step height). It can also be noted from Figure 24 that the value of C_v is directly proportional to the y_f/h_1 ratio for all tested models.

3.3. *Multi-variable regression models for C_d and C_v prediction*

A distinct multi-variable regression model has been derived to predict each of C_d and C_v. Therefore, the discharge and approach velocity coefficient values estimated for C_d and C_v, as obtained from the nine different compound cross-section types, were pooled together for the purpose of developing appropriate predictive regression models for both coefficients. Both derived prediction models are non-linear in form as indicated by Equations (11) and (12). For the C_d coefficient, the model has been derived as a function of 3 dimensionless parameters, namely, R_2, R_3, and R_4 as defined in Equation (11).

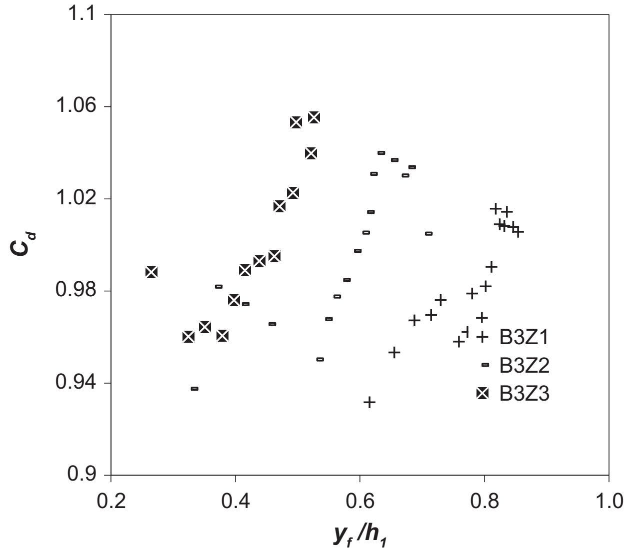

Figure 15. C_d vs. y_f/h_1 for varying step height and constant bottom width of the control section (b = 16 cm).

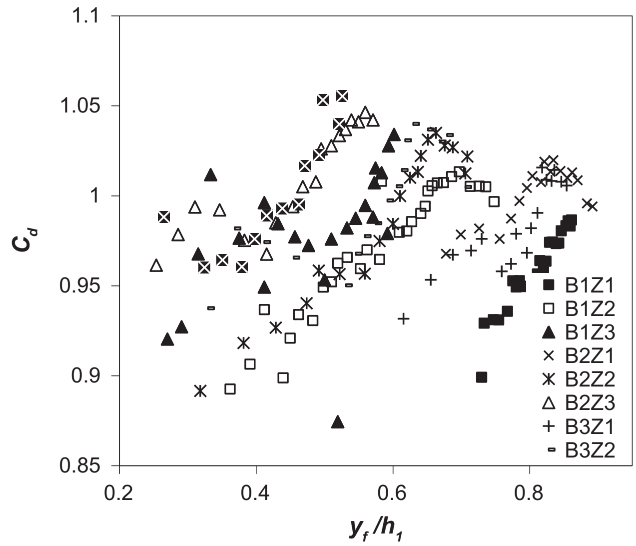

Figure 16. C_d vs. y_f/h_1 for all tested models.

$$\ln C_d = -0.244 - 0.026(R_2)(R_3) - 2.075(R_2)^6(R_3)^5 + 0.646[\mathrm{Sin}(R_4)] - 0.115(R_2)^8 - 0.239(R_4)^4 \tag{11}$$

where $R_2 = y_f/h_1$, $R_3 = B_o/b$, $R_4 = h_1/L_{\mathrm{thr}}$.

Similarly, the regression model to predict the C_v coefficient has been derived as a function of 3 dimensionless parameters, namely, R_1, R_2, and R_3 as presented in Equation (12). The parameter R_1 was defined in Equation (8) and used in Figure 17.

$$\ln C_v = 0.163 + 0.023(R_2)^8 - 1.18 \times 10^{-8}(R_3)^8 + 0.287(R_1)^9 - 0.001(R_1)^{-9} \tag{12}$$

The multi-variable linear regression techniques have been used to estimate the regression coefficients associated with the two derived multi-variable regression models after performing the necessary linear transformations. When deriving the generalized empirical models for C_d and C_v as presented in Equations (11) and (12), respectively, optimization of 5 main regression statistics was done to arrive at the best possible prediction regression equation. The estimated values of the 5 deployed statistics are provided in Table 2.

The corresponding variable coefficient t-statistic values are generally high ranging from 5.69 to 24.31 for C_d and from 3.69 to 98.09 for C_v, which results in a confidence level of 99.99%. The Variance Inflation Factor (VIF) which measures

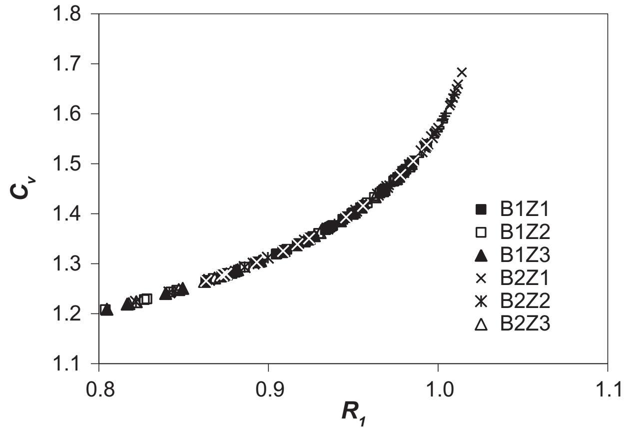

Figure 17. C_v vs. $R1$ for all tested models.

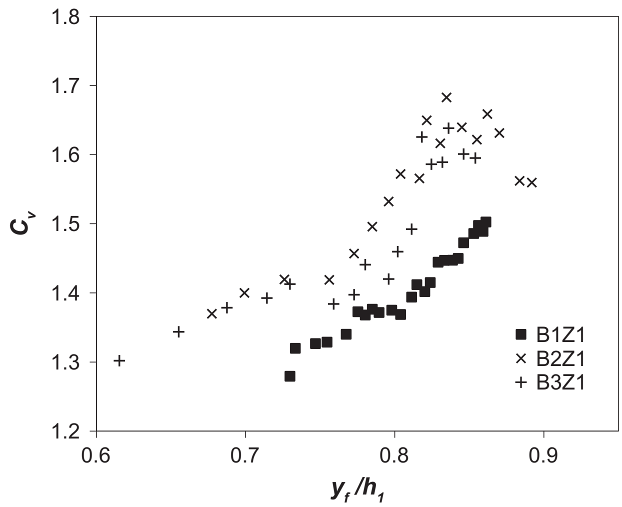

Figure 18. C_v vs. y_f/h_1 for varying bottom width of the control section and constant step height (Z = 2 cm).

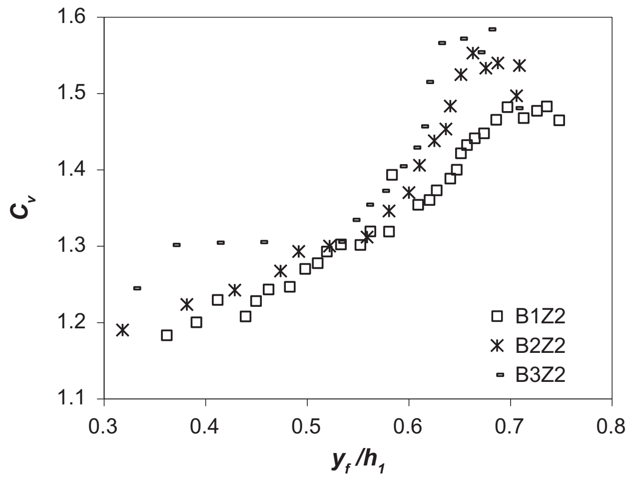

Figure 19. C_v vs. y_f/h_1 for varying bottom width of the control section and constant step height (Z = 6 cm).

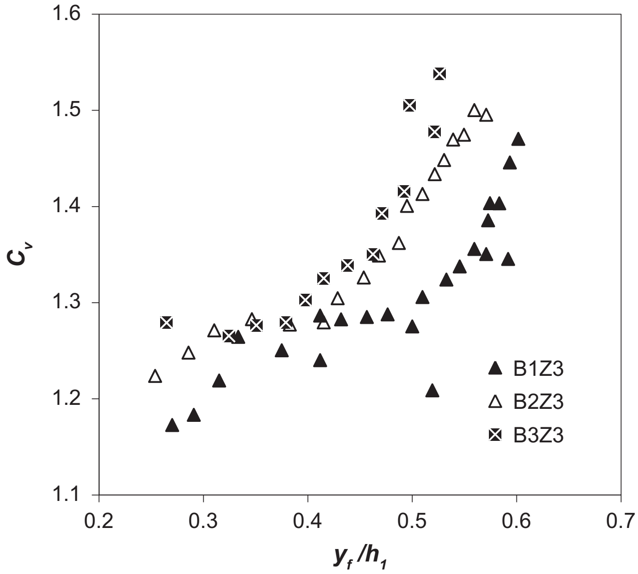

Figure 20. C_v vs/ y_f/h_1 for varying bottom width of the control section and constant step height (Z = 10 cm).

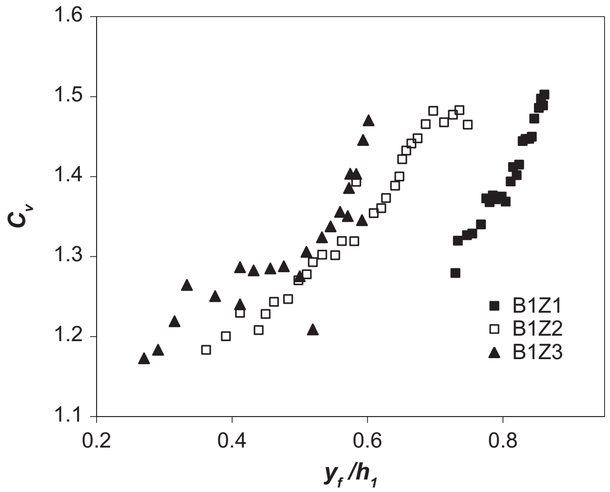

Figure 21. C_v vs. y_f/h_1 for varying step height and constant bottom width of the control section (b = 6 cm).

the impact of collinearity among the independent variables in a regression model on the precision of estimation is also provided in Table 2. It expresses the degree to which collinearity among the predictors degrades the precision of an estimate. Typically, a VIF value greater than 10 is of concern (Kutner et al. 2004). The provided values of the VIF indicate that none of them has exceeded the critical VIF value of 10. The empirical prediction models for C_d and C_v presented in Equations (11) and (12) are significant at a confidence level of 99.99% as the model F-statistic is equal to the value of 153.53 for C_d and 7788.65 for C_v as provided in Table 2. The predictive models have a determination coefficient (R-square) of 0.858 for C_d and 0.996 for C_v. The last statistic used is the model standard error of estimate which is generally small compared to the predicted C_d and C_v values with its value being equal to 0.0116 for C_d and 0.00014 for C_v.

In addition to the above five main statistics, a detailed analysis of the residuals associated with the two predicted variables ln C_d and ln C_v has been performed. The analysis includes the normal probability plots as provided in Figures 25 and 26 and the histograms of standardized residuals as presented in Figures 27 and 28. These plots generally show that there are no deviations from the assumptions of linearity, normality and constant variance for the error terms associated with the derived predictive models. Hence, it can be concluded that the regression models developed for C_d and C_v provide a good fit for the experimentally generated data. Finally, the developed regression models are validated using a holdout sample of about 40% of the total sample size to verify the models' predictive strength. The corresponding mean of the squared prediction errors (MSPR) has been calculated for both C_d and C_v with the results provided in Table 3. It is clear from Table 3 that the MSPR values associated with both regression models, as obtained from Equation (13), are very

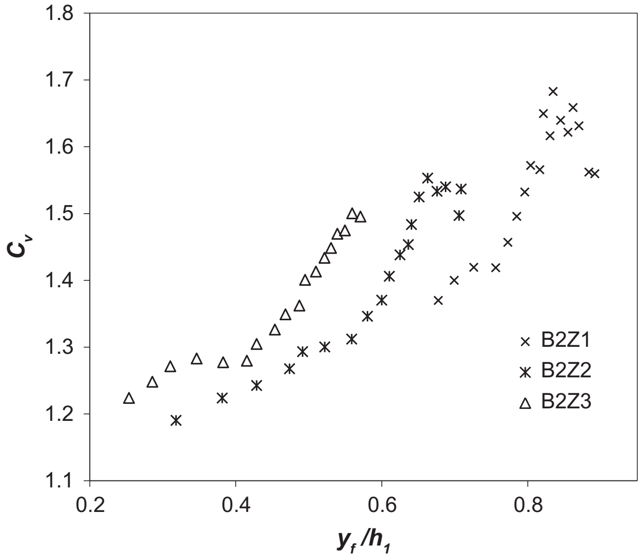

Figure 22. C_v vs. y_f/h_1 for varying step height and constant bottom width of the control section (b = 11 cm).

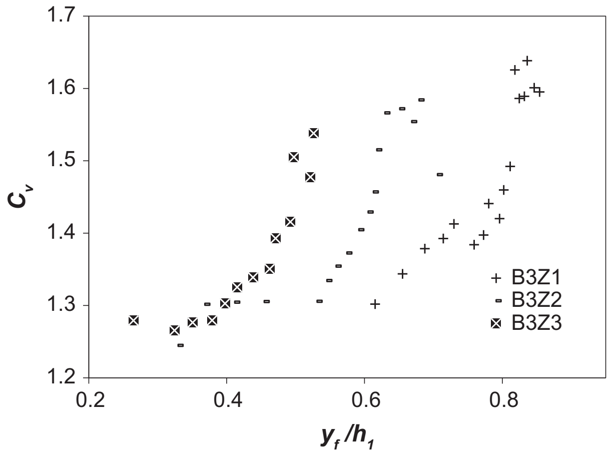

Figure 23. C_v vs. y_f/h_1 for varying step height and constant bottom width of the control section (b = 16 cm).

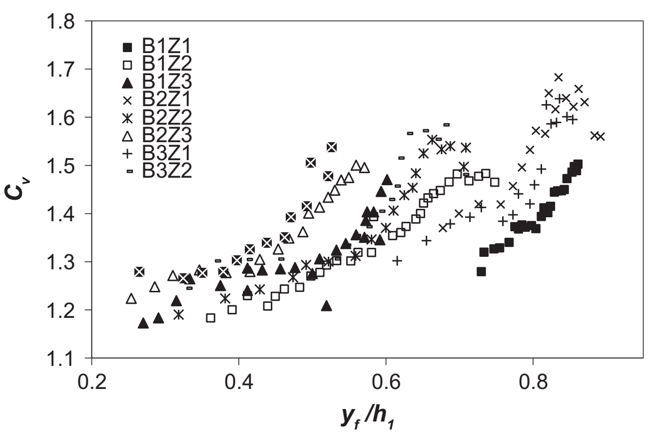

Figure 24. C_v vs. y_f/h_1 for all tested models.

Table 2. Summary of statistics associated with multi-variable regression predictive models.

Predicted variable	Model coefficients	Coefficient t-statistic	Confidence level (%)	Coefficient VIF	Model F-statistic	Model R-Square	Model standard error
Ln C_d	−0.244	−24.31	99.9	NA	153.53	0.858	0.0116
	−0.026	−16.64	99.9	2.689			
	−2.075	−6.17	99.9	2.276			
	0.646	24.07	99.9	7.741			
	−0.115	−5.69	99.9	4.118			
	−0.239	−11.06	99.9	6.528			
Ln C_v	0.163	67.85	99.9	NA	7788.6	0.996	0.00014
	0.023	4.02	99.9	1.818			
	-1.18×10^{-8}	−3.69	99.9	1.185			
	0.287	98.09	99.9	4.047			
	0.001	−3.86	99.9	2.695			

NA = Not applicable because the corresponding coefficient value is zero.

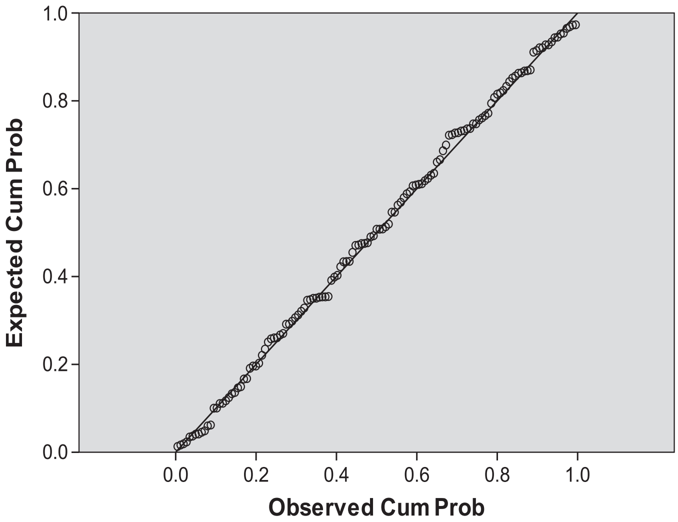

Figure 25. Normal p–p plot of expected vs. observed cumulative probabilities of residuals of (ln C_d).

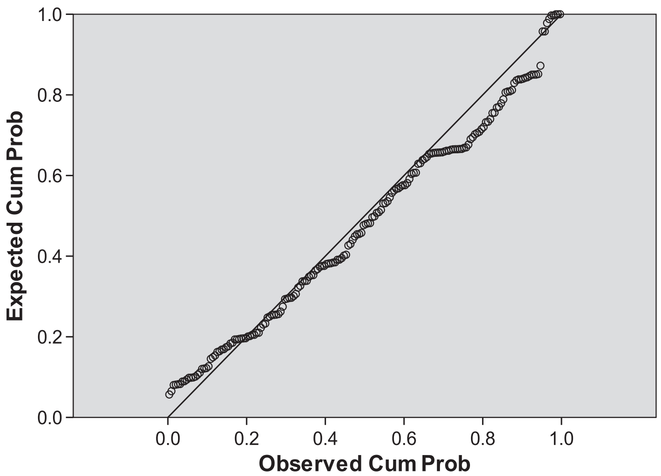

Figure 26. Normal p–p plot of expected vs. observed cumulative probabilities of residuals of (ln C_v).

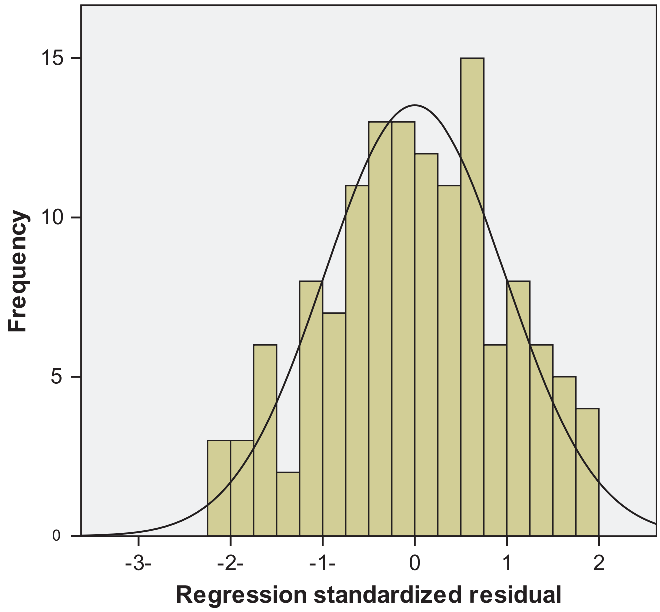

Figure 27. Histogram of standardized residuals for the dependent variable (ln C_d). [To view a colour version of this figure, see the online version of this Journal.]

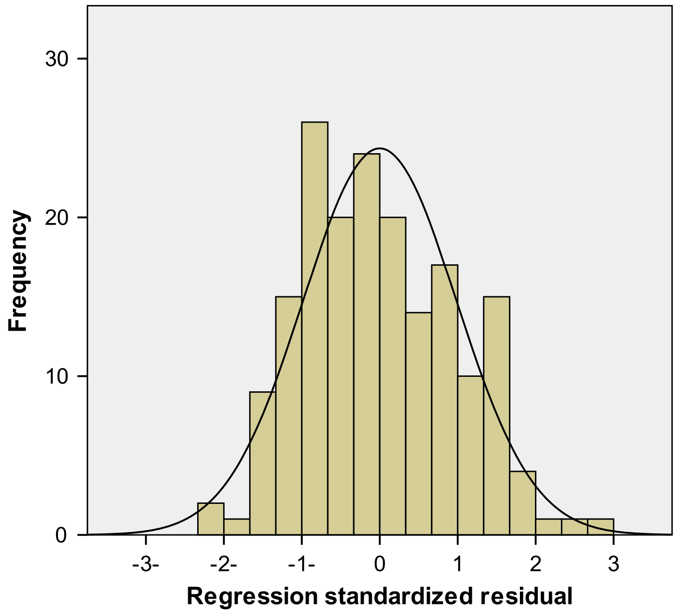

Figure 28. Histogram of standardized residuals for the dependent variable (ln C_v). [To view a colour version of this figure, see the online version of this Journal.]

Table 3. MSE and MSPR associated with the two multiple-variable regression models.

Dependent variable	MSE	MSPR
Ln Cv	0.0000283	0.0000242
Ln C_d	0.000119	0.000129

similar to their corresponding mean squared errors (MSE). This means that the MSE statistic is not seriously biased and it provides a good indication of the predictive ability of the two derived multi-variable regression models (Bos et al. 1984).

$$\mathrm{MSPR} = \frac{\sum_{i=1}^{n*} (Y_i - \hat{Y}_i)^2}{n*} \tag{13}$$

where Y_i = the value of the response variable in the ith validation case, $\hat{Y}_i$ = the predicted value of the response variable for the ith validation case based on the model-building data-set, and $n*$ = the number of cases in the validation data-set.

3.3.1. *Estimation of discharge from head measurement (h_1)*

The discharge can be predicted with high reliability for a given head h_1 using Equations (1) and (5) once the discharge and approach velocity coefficients (C_d and C_v) are estimated using the multi-variable regression models presented in Equations (10) and (11), respectively. Therefore, the discharge can be predicted using the measured h_1 with the estimated values of $C_{d,}$ C_v and the channel cross-section dimensions; B_{o}, b, Z. However, it must be pointed out that the regression models presented are only valid for dimensionless ratio values ($R_1 - R_4$) similar to those used in the development of these models. The four dimensionless ratios have been assigned specific value ranges; therefore, the effective application of the presented regression models for estimating flow in open channels requires using values for $R_1 - R_4$ that fall within the deployed value ranges. Similar regression models can be developed for predicting flow in natural rivers provided discharge data and cross-section geometry are available.

4. Conclusions

The discharge and approach velocity coefficients have been experimentally estimated and presented for nine different flow measurement long-throated flumes with symmetrical rectangular compound cross-section. The two coefficients are estimated from the stage-discharge equations using mainly head measurements and cross-section geometry. The relationships between the experimentally estimated coefficients and several dimensionless parameters are then investigated. The dimensionless parameters are mainly ratios defined using the flume geometric dimensions including throat length, head measurement section dimensions, and control cross-section dimensions.

It has been observed from all presented cases that the discharge and approach velocity coefficients are directly proportional to the y_f/h_1 ratio. In addition, the discharge coefficient has been found to be directly proportional to the h_1/L_{thr} ratio whereas the approach velocity coefficient is directly proportional to the area ratio ($\sqrt{\propto} C_d A^*/A_1$). An increase in the bottom width of the control section has resulted in an increase in the discharge coefficient after a critical h_1/L_{thr} value. A similar increase in the discharge coefficient has also been observed when increasing the step height past a critical h_1/L_{thr} value. The impacts of the control section bottom width and step height on the discharge coefficient in relation to the y_f/h_1 ratio are similar to their impacts when considering the h_1/L_{thr} ratio. The approach velocity coefficient is also directly proportional to the bottom width of the control section past a critical y_f/h_1 value. However, increasing the step height has minor effect on the approach velocity coefficient, but a large step height is associated with smaller y_f/h_1 values while a smaller step height is associated with larger y_f/h_1 values.

The above observations have greatly helped identifying the dimensionless parameters that should be used in developing the proposed multi-variable regression models for predicting the discharge and approach velocity coefficients. The proposed regression models are non-linear in form with each model using three relevant dimensionless parameters. These dimensionless parameters are only defined using the throat length, head measurement section dimensions, and control cross-section dimensions. The two proposed multi-variable regression models have been developed while using five key statistics as indicators of the model predictive strength. In general, the five deployed statistics have indicated the high reliability and significance of the two models in predicting the discharge and approach velocity coefficients. This has been also complemented and validated using a detailed analysis of residuals which indicated that the two predictive models provide a good fit of the experimentally estimated data. In summary, the paper main contribution is the derivation of two regression-based models for predicting flow using the discharge and approach velocity coefficients along with the stage discharge equations and channel cross-section dimensions.

Notation

A^*	imaginary wetted area at control section if water depth were equal to h_1
A_c	cross-sectional area of flow at critical depth-measurement section
A_1	cross-sectional area of flow at head measurement section
a	elevation difference between floor of test channel and invert of flume
B, Bi	bottom width of approach channel (i = 1, 2, 3)

B_c	top width of flow at control section
B_o	top width of head measurement section and weir model cross section
b	bottom width of the control section
C_d	discharge coefficient
C_v	approach velocity coefficient
g	acceleration of gravity
H_1	total energy head at upstream head measurement section
h_1	head at upstream head measurement section
L_{app}	length of approach channel
L_{ct}	length of converging transition
L_{dt}	length of diverging transition
L_{ent}	length of entrance channel
L_{thr}	length of throat in the direction of flow
MSE	mean squared errors
MSPR	mean of the squared prediction errors
n^*	the number of cases in the validation data-set
Q	volumetric rate of flow
Q_m	measured discharge
Q_p	predicted discharge
R-square	determination coefficient
R_1	$\sqrt{\propto} C_d A^*/A_1$
R_2	y_f/h_1
R_3	B_o/b
R_4	h_1/L_{thr}
V_c	average critical flow velocity at control section
VIF	Variance Inflation Factors
V_1	average flow velocity at upstream head measurement section
y_c	critical water depth at control section
y_f	$h_1 - Z$
Y_i	the value of the response variable in the ith validation case
$\hat{Y}_i$	the predicted value of the response variable for the ith validation case based on the model-building data-set
Z	step height of model cross section; and
α	energy correction coefficient
θ and β	entrance angles

References

Al-Khatib, I.A. (1989). "Hydraulic characteristics of flow measurement flumes of rectangular compound cross sections." M.Sc. thesis, Middle East Tech. University, Ankara, Turkey.

Al-Khatib, I.A. (1993). "Hydraulic characteristics and optimum design of symmetrical compound channels for flow measurements." Ph.D. dissertation, Middle East Tech. University, Ankara, Turkey.

Al-Khatib, I.A. (1999). "Modular limit for flumes of rectangular compound sections." *Turkish J. Eng. Environ. Sci.*, 23, 1–8.

Al-Khatib, I.A., Dweik, A.A., and Gogus, M. (2012). "Evaluation of separate channel methods for discharge computation in asymmetric compound channels." *Flow Meas. Instrum.*, 24, 19–25.

Boiten, W. (2002). "Flow measurement structures." *Flow Meas. Instrum.*, 13(5–6), 203–207.

Bos, M.G. (1977). "The use of long-throated flumes to measure flows in irrigation and drainage canals." *Agric. Water Manage.*, 1, 111–126.

Bos, M.G. (1989). *Discharge measurement structures*, 3rd edn, Wageningen, Publication 20. International Institute for Land Reclamation and Improvement. 401 pp.

Bos, M.G., and Reinink, Y. (1981). "Required head loss over long-throated flumes." *J. Irrigation and Drainage Div, ASCE*, 107(1), 87–102.

Bos, M.G., Replogle, J.A., and Clemmens, A.J. (1984). *Flow measuring flumes for open channel systems*, John Wiley and Sons, New York, NY.

Clemmens, A.J., Bos, M.G., and Replogle, J.A. (1987). "Contraction ratios for weir and flume designs." *J. Irrigation and Drainage Eng., ASCE*, 113(3), 420–424.

Clemmens, A.J., Replogle, J.A., and Bos, M.G. (1984). "Rectangular measuring flumes for lined and earthen channels." *J. Irrigation and Drainage Eng., ASCE*, 110(2), 121–137.

Clemmens, A.J., Wahl, T.L., Bos, M.G., and Replogle, J.A. (2001). *Water measurement with flumes and weirs*, vol. 58, Wageningen, International Institute for Land Reclamation and Improvement/ILRI Publication.

Emamgholizadeh, S., and Assare, K. (2008). "Investigation of the upstream and downstream slope of the long-throated flumes on the discharge coefficient." *J. Eng. Appl. Sci.*, 3(2), 62–70 (Asian Research Publishing Network).

Ghimire, B.N.S., and Reddy, M.J. (2010). "Development of stage-discharge rating curve in river using genetic algorithms and model tree." International Workshop: Advances in Statistical Hydrology, May 23–25, Taormina, Italy.

Göğüş, M., and Al-Khatib, I. (1995). "Flow measurement flumes of rectangular compound cross section." *J. Irrigation and Drainage Eng., ASCE*, 121(2), 135–142.

Göğüş, M., Defne, Z., and Özkandemir, V. (2006). "Broad-crested weirs with rectangular compound cross sections." *J. Irrigation and Drainage, ASCE*, 132(3), 272–280.

Gonzalez, C.A., and Chanson, H. (2007). "Experimental measurements of velocity and pressure distributions on a large broad-crested weir." *Flow Meas. Instrum.*, 18(3–4), 107–113.

Heiner, B., and Barfuss, S.L. (2011). "Parshall flume discharge corrections: wall staff gauge and centerline measurements." *J. Irrigation and Drainage Eng., ASCE*, 137(12), 779–792.

Kutner, M.H., Nachtsheim, C.J., and Neter, J. (2004). *Applied linear regression models*, 4th edn, Irwin, McGraw-Hill.

Sahu, M., Khatua, K.K., and Mahapatra, S.S. (2011). "A neural network approach for prediction of discharge in straight compound open channel flow." *Flow Meas. Instrum.*, 22, 438–446.

Unal, B., Mamak, M., Seckin, G., and Cobaner, M. (2010). "Comparison of an ANN approach with 1-D and 2-D methods for estimating discharge capacity of straight compound channels." *Adv. Eng. Softw.*, 41, 120–129.

Van Prooijen, B.C., Battjes, J.A., and Uijttewaal, W.S.J. (2005). "Momentum exchange in straight uniform compound channel flow." *J. Hydraul. Eng., ASCE*, 131(3), 175–183.

Vatankhah, A.R., and Mahdavi, A. (2012). "Simplified procedure for design of long-throated flumes and weirs." *Flow Meas. Instrum.*, 26, 79–84.

Wahl, T.L., Clemmens, A.J., Replogle, J.A., and Bos, M.G. (2000). "WinFlume - windows-based software for the design of long-throated measuring flumes." Fourth Decennial National Irrigation Symposium, American Society of Agricultural Engineers, Nov. 14–16, 2000, Phoenix, Arizona.

Wahl, T.L., Clemmens, A.J., Replogle, J.A., and Bos, M.G. (2005). "Simplified design of flumes and weirs." *Irrigation and Drainage*, 54(2), 231–247.